International Journal of Fatigue 61 (2014) 283–296

Contents lists available at ScienceDirect

International Journal of Fatigue

journal homepage: www.elsevier.com/locate/ijfatigue

Fatigue behavior of laser welds in lap-shear specimens of high strength low alloy steel sheets

Kamran Asim, Kulthida Sripichai, Jwo Pan *

Department of Mechanical Engineering, University of Michigan, Ann Arbor, MI 48109, United States

ARTICLE INFO

Article history:
Received 9 January 2011
Received in revised form 12 October 2013
Accepted 17 October 2013
Available online 26 October 2013

Keywords:
Laser weld
Lap-shear specimen
Kinked crack
Failure mode
Fatigue crack growth

ABSTRACT

In this paper, the fatigue behavior of laser welds in lap-shear specimens of non-galvanized SAE J2340 300Y high strength low alloy (HSLA) steel sheets is investigated based on experimental observations and a fatigue life estimation model. Optical micrographs of the laser welds before and after failure under quasi-static and cyclic loading conditions are examined. The micrographs show that the failure modes of laser welds under quasi-static and cyclic loading conditions are quite different. Under quasi-static loading conditions, the weld failure appears to be initiated from the base metal near the boundary of the base metal and the heat affected zone at a distance to the pre-existing crack tip, and the specimens fail due to the necking/shear of the lower left load carrying sheets. Under low-cycle loading conditions, the weld failure appears to be initiated from the pre-existing crack tips and the specimens finally fail from the ductile fracture through the lower left load carrying sheets. Under high-cycle loading conditions, the weld failure appears to be initiated from the pre-existing crack tips and the specimens finally fail from the kinked fatigue crack propagating through the upper right load carrying sheets. Finite element analyses of the laser welded lap-shear specimens with consideration of the weld bead protrusion were carried out to obtain the global and local stress intensity factor solutions for the main cracks and kinked cracks, respectively. The stress intensity factor solutions can be used to explain the kinked fatigue crack growth patterns under high-cycle loading conditions. The kinked fatigue crack growth model based on the global and local stress intensity factor solutions for finite kinked cracks obtained from the finite element analyses is adopted to estimate the fatigue lives of the laser welds. The fatigue life estimations based on the kinked fatigue crack growth model agree well with the experimental results.

1. Introduction

Laser welding has many advantages over the conventional welding methods. These advantages include relatively low distortion of the weld, narrow heat affected zone, relatively high welding speed and high penetration. Over the past two decades, extensive research efforts have been spent on studying the fatigue behavior of laser welds for different materials and joint configurations. Lap joints have been commonly used to assess the strength and fatigue behavior of laser welds under shear dominant loading conditions. The geometry of a lap joint provides pre-existing cracks or notches at the edges of the weld bead. Therefore, the fatigue cracks were usually observed to be initiated from these stress concentration sites. Hsu and Albright [1] combined a static stress analysis and Neuber's rule to predict the fatigue lives of laser welded lap joints. Wang and Ewing [2] compared the fatigue strengths of laser welds and resistance spot welds in lap-shear specimens of steel sheets on the basis of equal weld volume. They reported that the fatigue failure in laser welds is dominated by crack propagation in the heat affected zone. Flavenot et al. [3] performed an experimental study to examine the influence of laser beam type, weld bead geometry, gap between the sheets and the input energy on the fatigue behavior of laser welded lap joints. Wang [4] correlated the experimental fatigue lives of laser welds in lap-shear specimens with the values of the J integral obtained from finite element analyses. The results were also used to assess the influence of parameters such as the weld geometry, sheet thickness, bead width, metal fit-up and bead length. Ono et al. [5] investigated the static and fatigue strengths of laser welded lap joints of thin steel sheets and correlated the fatigue lives of laser welded lap joints with the maximum stress intensity factor ranges.

Terasaki et al. [6] examined the fatigue lives of laser welded lap joints and correlated the experimental results by the stress intensity factor solutions. Zhang [7] proposed structural stress solutions based on the outer surface strains of laser welded lap joints. Kaitanov et al. [8] conducted experiments to determine the static and fatigue strengths of laser welded lap joints of steel sheets with different weld widths and penetration depths. They found that the weld width affects the fatigue strength of laser welds. Cho et al.

* Corresponding author. Tel.: +1 734 764 9404; fax: +1 734 647 3170.
E-mail address: jwo@umich.edu (J. Pan).

0142-1123/$ - see front matter © 2013 Elsevier Ltd. All rights reserved.
http://dx.doi.org/10.1016/j.ijfatigue.2013.10.019

[9] examined the fatigue strength of laser welded lap joints with the consideration of residual stresses obtained from thermo-mechanical finite element analyses. Sripichai et al. [10] investigated the fatigue behavior of laser welds in lap-shear specimens of high strength low alloy steel sheets based on the closed-form and computational stress intensity factor solutions.

In this study, the fatigue behavior of laser welds in lap-shear specimens of non-galvanized SAE J2340 300Y HSLA steel sheets is investigated based on experimental observations and a fatigue life estimation model. Optical micrographs of the welds before and after failure under quasi-static and cyclic loading conditions are examined to investigate the microstructure and failure mechanisms of the welds. Scanning electron micrographs of the failure surfaces are also used to explain the failure modes of laser welds in lap-shear specimens under quasi-static and cyclic loading conditions. Finite element analyses of the laser welded lap-shear specimens with consideration of the weld bead protrusion were carried out to obtain the global and local stress intensity factor solutions for the main cracks and kinked cracks, respectively. The stress intensity factor solutions are used to explain the kinked fatigue crack growth patterns under high-cycle loading conditions. The kinked fatigue crack growth model based on the global and local stress intensity factor solutions for finite kinked cracks obtained from the finite element analyses is adopted to estimate the fatigue lives of the laser welds. The estimated fatigue lives are compared with the experimental results.

2. Experiment

HSLA steel sheets with a thickness of 0.93 mm were used in this investigation. The mechanical properties obtained from the tensile tests of the HSLA steel sheets are listed in Table 1. The sheets were welded using CO_2 laser with an output power of 6 KW. The laser beam was held stationary while the sheets were moved at a speed of 8 m/min in the welding direction. Helium was used as the shielding gas with a discharge rate of 20 ℓ/min. The welded sheets were then sheared into 27 mm wide strips with a length of 275 mm. These sheet strips were machined into specimens with a dog-bone shaped profile using a CNC milling machine according to the guidelines provided in the ANSI/AWS B4.0:2007 standard for mechanical testing of welds and the ASTM E466-07 standard for conducting force controlled constant amplitude axial fatigue tests of metallic materials. After machining, the specimen edges were manually smoothed by using 1200 grit coarse polishing papers. This was done to remove any notches or irregularities along the edges which may produce stress concentration sites. Figs. 1(a) and (b) show top and bottom views of a laser welded lap-shear specimen, respectively.

The geometry of the specimen was chosen to avoid failure due to the necking of the sheets far from the weld zone and to allow an investigation of the failure mechanism in the vicinity of the laser weld. Specimens with similar shapes were used for the study of laser welded joints, for example, see, Anand et al. [11] and Sripichai et al. [10]. Fig. 2 shows a schematic of a lap-shear specimen. As shown in the figure, the specimen has a width W, sheet thickness t, and length L for the upper and lower sheets. The specimen has a width b and a length c for the central portion of the specimen,

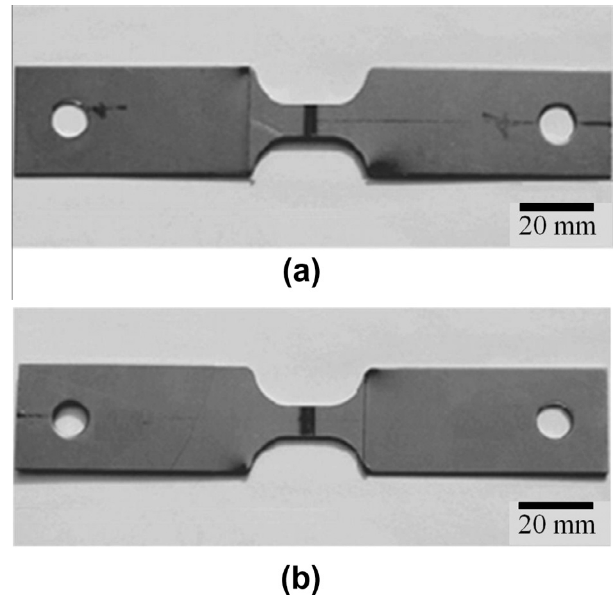

Fig. 1. (a) A top view and (b) a bottom view of a laser welded lap-shear specimen.

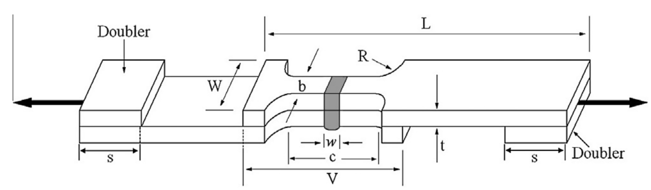

Fig. 2. A schematic of a lap-shear specimen with the loading directions shown as the bold arrows.

an overlap length V, and a width w for the weld zone, which is indicated as the shaded region in the figure. Two doublers were used to align the applied load to avoid the initial realignment of the specimen under lap-shear loading conditions. The doublers have a length s and a width W. The detailed dimensions of the lap-shear specimen are listed in Table 2. The loading direction is indicated by two bold arrows on the left and right sides of the specimen in the schematic. The bold arrows are used to indicate the loading directions in the subsequent figures.

Fig. 3(a) shows an optical micrograph of the etched cross section of a laser weld in a lap-shear specimen perpendicular to the welding direction before testing. Based on their distinct grain structures, three separate regions can be identified from the micrograph, namely, the base metal with equiaxed fine grains, the heat affected zone (HAZ) with fine and coarse grains, and the fusion zone with columnar grains. The width of the fusion zone, as seen from the micrograph in Fig. 3(a), is about 0.80 mm along the middle surface of the weld between the two pre-existing cracks. The width of the HAZ, as shown in the micrograph in Fig. 3(a), is about 0.05 to 0.17 mm on both sides of the fusion zone from the top to

Table 1
Mechanical properties from the tensile tests of HSLA base metal sheets.

Elastic modulus (GPa)	Yield strength (MPa)	Tensile strength (MPa)	Hardening exponent, n	Strength coefficient, K (MPa)
206	315	415	0.15	633

Table 2
Dimensions of the lap-shear specimen.

Width of the grip section (W)	27.0 mm
Width of the central portion (b)	8.0 mm
Length of the central portion (c)	13.5 mm
Weld width (w)	1.0 mm
Length of each leg (L)	95.0 mm
Sheet overlap length (V)	30.0 mm
Sheet thickness (t)	0.93 mm
Radius (R)	10.0 mm
Length of the doubler (s)	50.0 mm